SUPPLEMENTARY INFORMATION

Lanthanide Nanoparticles as Ultra-Sensitive Luminescent Probes for Quantitative PSA Detection via Lateral Flow Assays.

Table of content

Experimental section

Reagents

Mouse anti-human PSA monoclonal antibodies and standard PSA were purchased from Revvity (Waltham, MA, USA). Goat anti-mouse IgG polyclonal antibody was purchased from Abliance (Compiègne, France). Now-Dtech™ – TR-FRET assay kit Mouse IgG was supplied by Poly-Dtech (Strasbourg, France). Recombinant Human Kallikrein 2 (hK2) protein was purchased from R&D systems (Minneapolis, Minnesota, USA).

Materials

Glass fibre sample membrane (ST17), backing card and absorbent pad (CF7) were purchased from Cytiva (Marlborough, MA, USA). Nitrocellulose membrane was purchased from Sartorius (Göttingen, Germany).

Instruments

The Agismart Rapid Test Printer-RP2000 (Rega Biotechnology INC., New Tapei City, Taiwan) was used to print test and control lines onto the nitrocellulose membrane. The strips were then cut with a strip cutter (AntiTeck Life Sciences, Guangzhou, China). A Mini Tube Rotator (Boekel Scientific, Feasterville, PA, USA) was employed for nanoparticle-antibody conjugation. The transmission electron microscopy (TEM) images were acquired on a JEOL 2100F electron microscope at 200 kV, equipped with a GATAN GIF 200 electron imaging filter. TECAN Spark microplate reader was used to characterize the excitation and emission spectra of the Bright-Dtech™ 614 – Eu nanoparticles (EuNPs). Dynamic Light Scattering (DLS) measurements were performed on an AMERIGO™ particle size & zeta potential analyser from Cordouan Technologies, equipped with a VASCO KIN™ particle size analyser for the measurements of DLS diameters.

Experimental Procedures

For TEM images, a drop of the nanoparticle's suspension was deposited onto TEM grids prepared with a porous membrane coated with an amorphous carbon layer. Only Bright-Dtech™ – 614 EuNPs located on the strand edges of membrane holes were analysed to minimize background noise from the amorphous carbon. Images were processed using ImageJ software, and core diameters were measured on approximately 100 nanoparticles. The straight-line tool was used to measure nanoparticle diameters from edge to edge.

Recombinant human kallikrein-2 (hK2) was used to assess specificity because of its close structural homology to PSA. Serum from three healthy donors was diluted 1:8 in assay buffer (0.25% BSA, 6.85 mM NaCl, 0.025% Tween-20). PSA was spiked into diluted serum at 0, 0.5, 5 and 50 ng/mL. hK2 was spiked either alone (0, 5, 50 and 500 ng/mL) to assess direct cross-reactivity or together with PSA (PSA 0, 0.5, 5, 50 ng/mL; hK2 0, 5, 50, 500 ng/mL) to assess competitive interference. For the spike-and-recovery experiment, PSA was spiked at the same levels into serum with or without high hK2 (500 ng/mL) and measured; recovery (%) was calculated as measured/expected ×100. The effect of the competing/interfering protein was assessed by calculating the percent change in PSA signal relative to PSA alone; interference (%) was calculated as measured-spiked/spiked x100. All conditions were run in triplicate (n = 3).

Tables

Table S1. Analytical parameters of the EuNPs-based LFA for PSA detection in buffer.

LOD (ng/mL)	LOQ (ng/mL)	Hillslope	EC_{50} (ng/mL)	DLR (ng/mL)	R^2
0.015	0.155	1.674	13.52	0.155-27.5	1.000

Abbreviations: Limit of detection (LOD), limit of quantification (LOQ), EC_{50}, dynamic linear range (DLR).

Figures

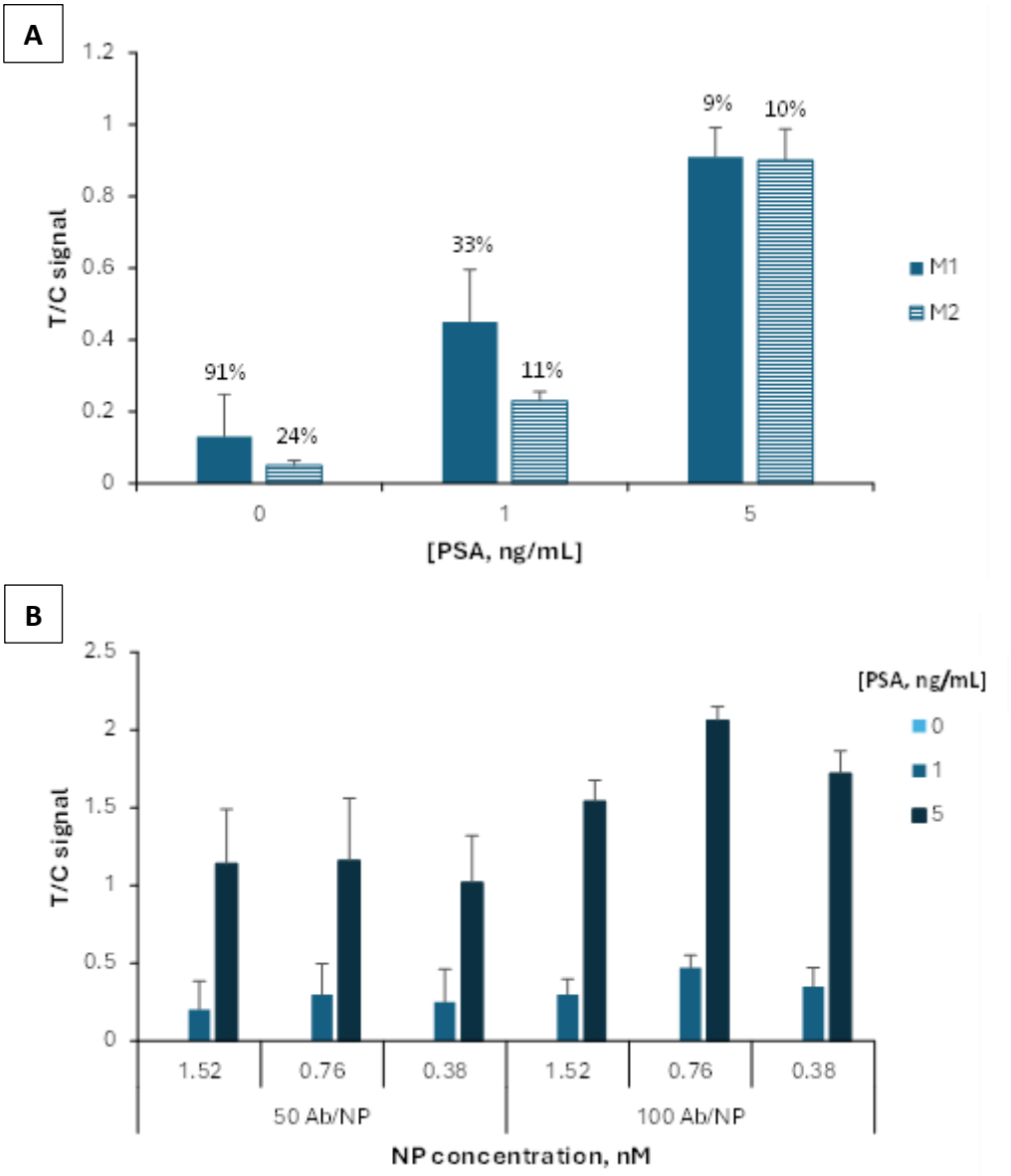

Fig. S1. Optimization of the LFA. (A) Evaluation of two nitrocellulose membranes (M1 and M2) for the detection 0, 1, and 5 ng/mL PSA in migration buffer. The value displayed above each bar represents the coefficient of variation (CV) in percentage (n=3). The two membranes tested, referred to as M1 and M2 differ in terms of porosity and migration speed, with M2 exhibiting faster flow characteristics. Membrane M2 was selected as it demonstrated lower non-specific interactions compared to membrane M1, indicated by a reduced background signal in the blank condition (0 ng/mL PSA), thereby providing a higher signal-to-noise ratio. Additionally, the lower CVs obtained with M2 reflect improved assay reproducibility. (B) Evaluation of three nanoparticle concentrations (1.52, 0.76, and 0.38 nM), each with either 50 or 100 anti-PSA antibody molecules per EuNP, for the detection of 0, 1, and 5 ng/mL PSA in migration buffer (n=3). The concentration of 0.76 nM EuNPs and a coupling ratio of 100 antibodies per EuNP produced the most pronounced signal difference between 0 and 1 ng/mL PSA. This condition was therefore selected for all subsequent experiments.

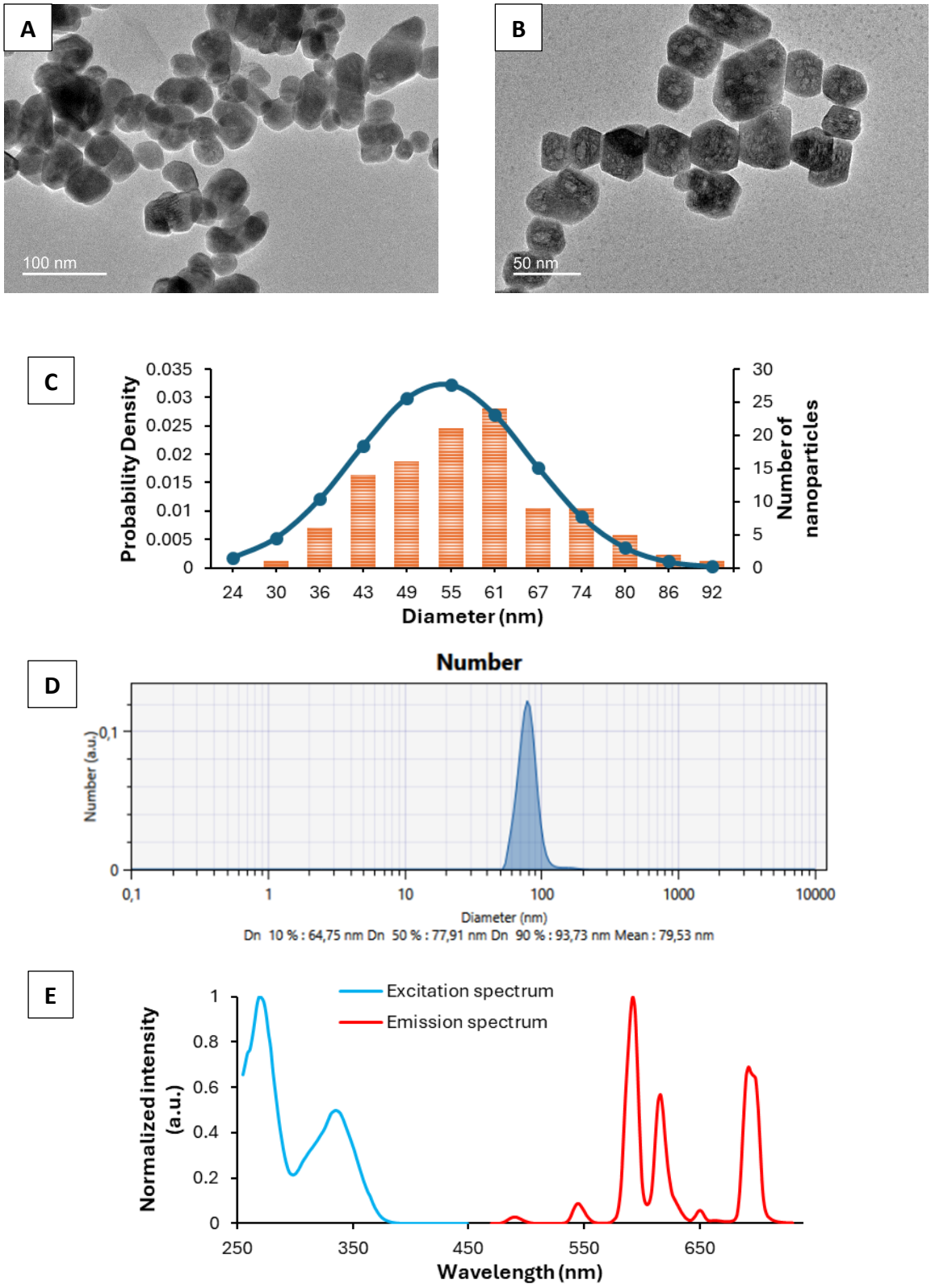

Fig. S2. Characterization of the Bright-Dtech™ 614 – EuNPs. (A, B) TEM images of the nanoparticles at two different magnifications. (C) Size distribution (blue curve represents probability density and orange histogram represents the number of nanoparticles by size, n=100). TEM analysis revealed that the EuNPs were spherical, with a diameter under 100 nm. The size distribution histogram demonstrated a homogeneous dispersion, with an average diameter of 53 ± 12 nm. (D) Hydrodynamic size measurements using Dynamic Light Scattering (DLS) revealing an average diameter of 79.53 nm. (E) Excitation and emission spectra. Optical characterization of the EuNPs revealed two excitation peaks at 340 and 280 nm. Upon excitation at 340 nm, three sharp emission peaks were observed at 590 nm, 614 nm, and 690 nm, with the highest fluorescence intensity observed at 590 nm.

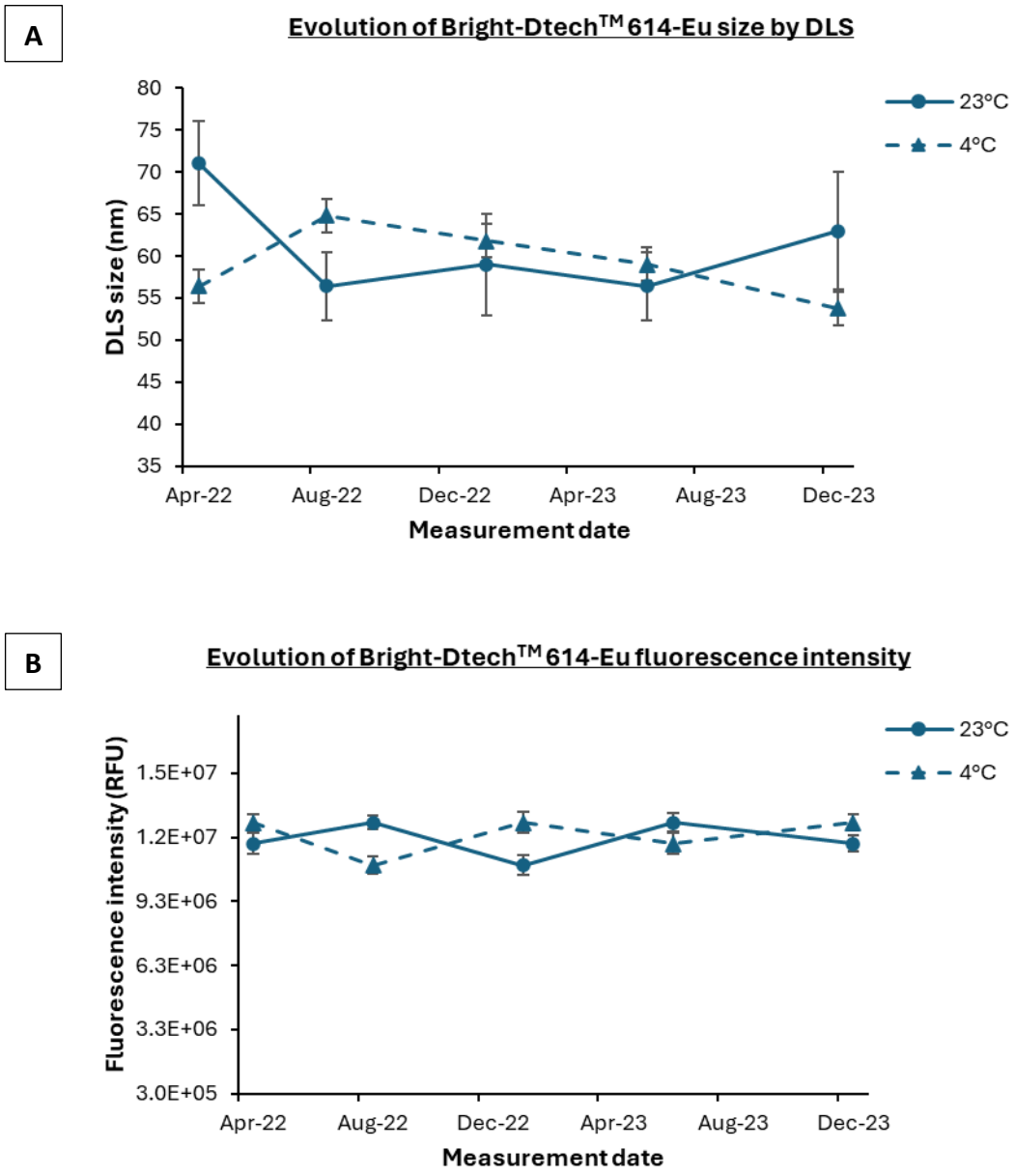

Fig. S3. Stability assessment of Bright-Dtech™ 614 - EuNPs. (A) Hydrodynamic size measurements using Dynamic Light Scattering (DLS), and (B) fluorescence intensity measurements were performed over a two-year period, with storage at both 23°C and 4°C. Fluorescence emission was measured at 616 nm using an appropriate bandpass filter, following excitation at 340 nm under time-resolved fluorescence conditions. The results show no significant changes in nanoparticle size or fluorescence intensity between the two storage temperatures, indicating that the nanoparticles maintain long-term stability under the tested conditions.

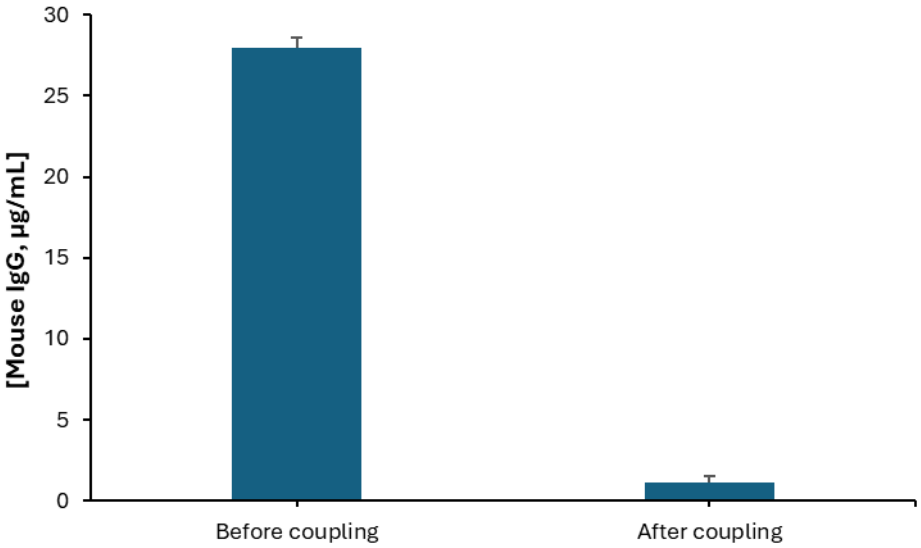

Fig. S4. Assessment of antibody conjugation efficiency. Residual mouse IgG levels in the supernatant after conjugation were quantified using a TR-FRET assay kit. The calculated conjugation efficiency was approximately 96 %, indicating successful antibody coupling to the nanoparticles.

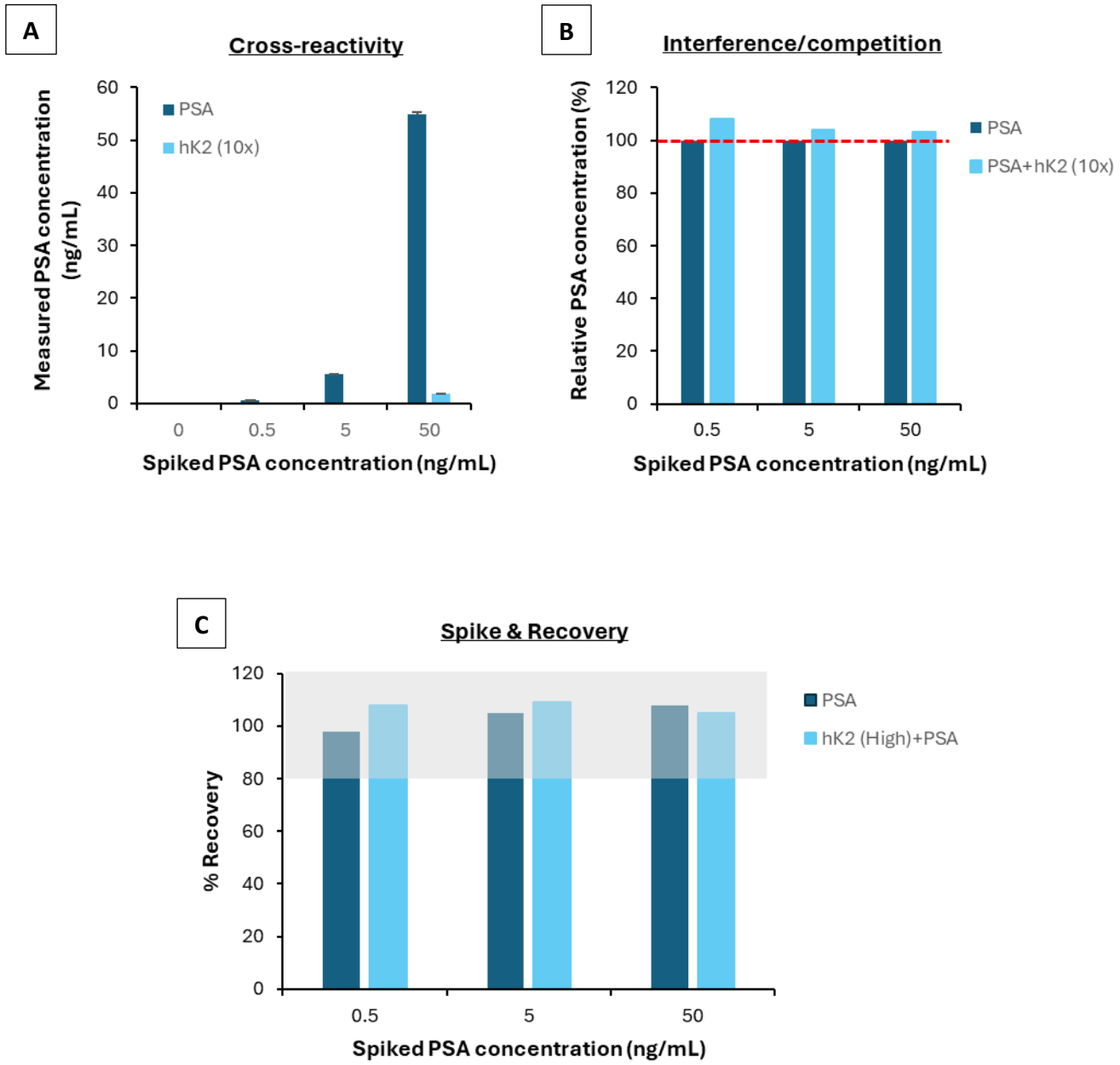

Fig. S5. Specificity assessment of the PSA LFA. (A) Cross-reactivity. Human serum was spiked with PSA (0, 0.5, 5, 50 ng/mL; dark blue bars) or with recombinant hK2 at 10-fold molar excess (0, 5, 50, 500 ng/mL; light blue bars) (n=3). Only PSA generated a measurable signal. hK2 responses overlapped with the blank (unspiked serum), except at the highest concentration tested (500 ng/mL), where a minor apparent signal corresponding to 2% cross-reactivity was detected. This value remains insignificant and confirms negligible cross-reactivity. (B) Interference/competition. PSA concentrations (0, 0.5, 5 and 50 ng/mL) measured in serum alone (dark blue bars) or in the presence of a 10x molar excess of hK2 (0, 5, 50, 500 ng/mL; light blue bars) (n=3). Normalized concentrations are shown relative to PSA alone (red dashed line = 100%). No significant increase was observed (8% for 0.5 ng/mL PSA, 4% for 5 ng/mL PSA and 3% for 50 ng/mL PSA), confirming the absence of competitive interference. (C) Spike-and-recovery. PSA recovery rates (measured concentration / expected concentration ×100) in serum alone (dark blue bars) and in serum supplemented with high hK2 (500 ng/mL; light blue bars) (n=3). All values remained within the predefined acceptance range of 80–120% (grey shaded area), indicating robust accuracy even in the presence of abundant non-target proteins.